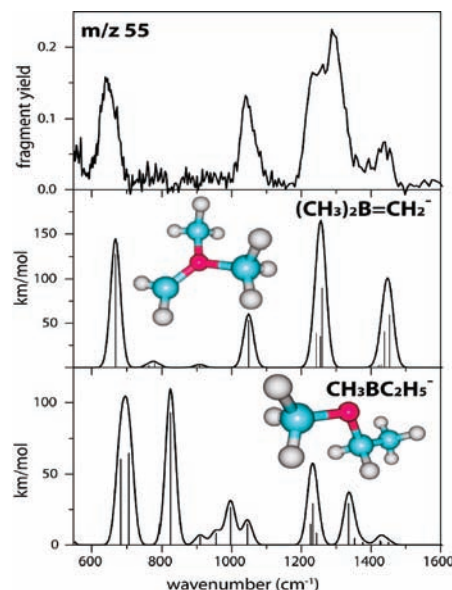


**Figure 1.** Experimental IRMPD spectrum of the gaseous fluoro-trimethylborate anion (upper panel) compared with the theoretical spectrum predicted for structure **2** by an unscaled B3LYP/aug-cc-pVTZ anharmonic calculation (lower panel) using harmonic intensities.<sup>7</sup>

Anion **2**, the fluoride adduct of **1** ( $m/z$  75 for the isotope  $^{11}\text{B}$ ), was formed in the external source of an FT-ICR mass spectrometer by electron ionization of a mixture of **1** and  $\text{SF}_6$ ,<sup>8</sup> then injected into the ICR cell, and isolated by a set of SWIFT ejection pulses to remove other ions.<sup>10</sup> Infrared resonant multiple photon dissociation (IRMPD) of **2** using the free-electron laser FELIX<sup>11</sup> leads to expulsion of HF, yielding an  $m/z$  55 anion. Monitoring disappearance of **2** simultaneously with the appearance of  $m/z$  55 as a function of wavelength gives the gas-phase IRMPD spectrum reproduced in the upper panel of Figure 1, which matches the DFT-calculated spectrum<sup>12</sup> in the lower panel.

Theoretical band positions (B3LYP with anharmonic corrections) match those of the experimental IRMPD. The largest discrepancy occurs for the symmetric methyl rock (calculated at 709 and seen at  $725\text{ cm}^{-1}$ ). The symmetric breathing mode (calculated at 606 and seen at  $597\text{ cm}^{-1}$ ) has a predicted harmonic intensity 2 orders of magnitude less than is observed. The biggest experimental band corresponds to three closely spaced vibrations with substantial BC stretching character. It is seen near  $1000\text{ cm}^{-1}$ , not far from the fundamental of a  $\text{CO}_2$  laser.

The question then arises as to the structure of the  $m/z$  55 ion produced by HF loss. Two alternative isomers seem possible: either the product of simple vicinal elimination,  $\text{Me}_2\text{BCH}_2^-$  (**3**), or a rearranged structure,  $\text{MeBCH}_2\text{CH}_3^-$ .<sup>13</sup> To probe the structure of gaseous  $\text{BC}_3\text{H}_8^-$ , ion **2** was stored for several seconds in the ICR and irradiated by the output of a quasi-cw  $\text{CO}_2$  laser. Infrared photolysis converts **2** nearly quantitatively via HF loss to the  $m/z$  55 anion, whose IR spectrum was then determined by resonant IR multiple photon electron detachment using the free electron laser.



**Figure 2.** Experimental IRMPD spectrum of the conjugate base anion of trimethylboron (top panel) compared with spectra calculated for structure **3** (middle panel) and for  $\text{MeBCH}_2\text{CH}_3^-$  (bottom panel) using unscaled B3LYP/aug-cc-pVTZ anharmonic calculations with harmonic intensities.<sup>7</sup>

Frequency-dependent electron detachment from  $\text{BC}_3\text{H}_8^-$  was monitored by production of  $\text{SF}_6^-$  and  $\text{F}^-$  from electron attachment to traces of  $\text{SF}_6$  in the ICR cell,<sup>14</sup> as well as by disappearance of  $m/z$  55. Figure 2 reproduces the IRMPD spectrum, along with the theoretically predicted spectra of  $\text{Me}_2\text{BCH}_2^-$  ( $C_2$ , symmetry) and of  $\text{MeBCH}_2\text{CH}_3^-$  ( $C_1$  symmetry). The absence of strong absorptions between 700 and  $1000\text{ cm}^{-1}$  shows that  $m/z$  55 does not have the  $\text{MeBCH}_2\text{CH}_3^-$  structure. The pronounced band seen near  $1440\text{ cm}^{-1}$  is consistent with predictions for the  $sp^2$ - $sp^2$  B=C bond of the  $\text{Me}_2\text{BCH}_2^-$  anion, **3**: a pair of overlapping  $A_1$  bands at 1439 and  $1454\text{ cm}^{-1}$ , corresponding to the B=C stretch coupled with three HCH scissor vibrations.

Table 1 lists experimental frequencies for ions **2** and **3** along with assignments based on animation of calculated peaks. Theory gives an excellent fit to the experimental peak positions, the biggest discrepancy being the bands of **3** corresponding to the CBC symmetric stretch coupled with the B=C stretch and methyl umbrella motions. The two  $A_1$  CBC stretches are predicted to be closer together ( $1260$  and  $1243\text{ cm}^{-1}$ ) than seen experimentally ( $1292$  and  $1235\text{ cm}^{-1}$ ), even though the antisymmetric combination of methyl umbrella motions (the  $B_1$  mode seen at  $1262\text{ cm}^{-1}$ ) occurs not far from where it is calculated ( $1255\text{ cm}^{-1}$ ).

Correspondence between experiment and theory warrants the use of DFT (B3LYP/aug-cc-pVTZ, the computational level used to predict the spectra in Figures 1 and 2) to look at the isoelectronic series in Scheme 1. Vibrational spectra of the gaseous cations<sup>15,16</sup> and neutrals<sup>17</sup> are published. In this series **1** and the carbocations are isoelectronic; anion **2** and

(10) Marshall, A. G.; Wang, T. C. L.; Ricca, T. L. *J. Am. Chem. Soc.* **1985**, *107*, 7893–7897.

(11) (a) Oepts, D.; van der Meer, A. F. G.; van Amersfoort, P. W. *Infrared Phys. Technol.* **1995**, *36*, 297–308. (b) Polfer, N. C.; Oomens, J. *Phys. Chem. Chem. Phys.* **2007**, *9*, 3804–2817.

(12) Frisch, M. J.; et al. *Gaussian 03*, Revision C.02.

(13) B3LYP/aug-cc-pVTZ geometry optimizations give electronic energies of  $-144.066617\text{ au}$  and  $-143.982025\text{ au}$  for ion **3** and  $\text{MeBCH}_2\text{CH}_3^-$ , predicting the former to be  $\approx 222\text{ kJ mol}^{-1}$  more stable than the latter.

(14) Steill, J. D.; Oomens, J. *J. Phys. Chem. A* **2009**, *113*, 4941–4946.

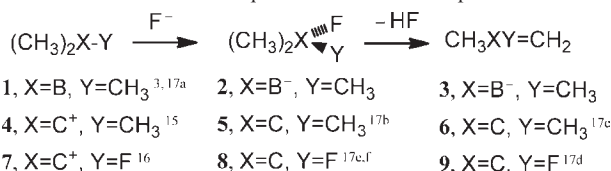
(15) Douberly, G. E.; Ricks, A. M.; Ticknor, B. W.; Schleyer, P. v. R.; Duncan, M. A. *J. Am. Chem. Soc.* **2007**, *129*, 13782–13783.

(16) Oomens, J.; Morton, T. H. *Angew. Chem., Int. Ed.* **2008**, *47*, 2106–2108.

(17) (a) Lehmann, W. J.; Wilson, C. O., Jr.; Shapiro, I. *J. Chem. Phys.* **1959**, *31*, 1071–1075. (b) Mann, D. E.; Acquista, N.; Lide, D. R., Jr. *J. Mol. Spectrosc.* **1958**, *2*, 575–580. (c) Pathak, C. M.; Fletcher, W. H. *J. Mol. Spectrosc.* **1969**, *31*, 32–53. (d) Crowder, G. A.; Smyrl, N. *J. Mol. Spectrosc.* **1971**, *40*, 117–124. (e) Crowder, G. A.; Jackson, D. *Spectrochim. Acta* **1971**, *27A*, 2505–2511. (f) Durig, J. R.; Guirgis, G. A.; Li, Y. S. *J. Chem. Phys.* **1981**, *74*, 5946–5953.

**Table 1.** Prominent IR Absorption Bands in the 600–1800 cm<sup>-1</sup> Domain Observed in the Experimental Spectra of Fluorotrimethylborate Anion (**2**) and the Conjugate Base of Trimethylboron (**3**) in the Gas Phase

| (CH <sub>3</sub> ) <sub>3</sub> BF <sup>-</sup> ( <b>2</b> , C <sub>3</sub> symm) |                                                                          | (CH <sub>3</sub> ) <sub>2</sub> BCH <sub>2</sub> <sup>-</sup> ( <b>3</b> , C <sub>2v</sub> symm) |                                                                          |
|-----------------------------------------------------------------------------------|--------------------------------------------------------------------------|--------------------------------------------------------------------------------------------------|--------------------------------------------------------------------------|
| obsd                                                                              | assignment                                                               | obsd                                                                                             | assignment                                                               |
| 1235                                                                              | CH <sub>3</sub> umbrella ( <i>A</i> )                                    | 1437                                                                                             | B=C stretch/HCH scissor ( <i>A</i> <sub>1</sub> )                        |
| 1222                                                                              | CH <sub>3</sub> umbrella ( <i>E</i> )                                    | 1292                                                                                             | CBC/B=C stretch/CH <sub>3</sub> umbrella ( <i>A</i> <sub>1</sub> )       |
| 1012                                                                              | CBC asym stretch ( <i>E</i> ) and BMe <sub>3</sub> umbrella ( <i>A</i> ) | 1262                                                                                             | CBC asym stretch/CH <sub>3</sub> umbrella ( <i>B</i> <sub>2</sub> )      |
| 725                                                                               | Sym CH <sub>3</sub> rock ( <i>A</i> )                                    | 1235                                                                                             | CBC/B=C stretch/CH <sub>3</sub> umbrella ( <i>A</i> <sub>1</sub> )       |
| 597                                                                               | Sym breathing ( <i>A</i> )                                               | 1045                                                                                             | CBC asym stretch/CH <sub>2</sub> in-plane bend ( <i>B</i> <sub>2</sub> ) |
|                                                                                   |                                                                          | 649                                                                                              | CH <sub>3</sub> out-of-plane wag ( <i>B</i> <sub>1</sub> )               |

**Scheme 1.** Isoelectronic Sequences for Which IR Spectra Are Known

the neutral, saturated molecules are isoelectronic; and anion **3** and the neutral alkenes are isoelectronic.

Kraka and Cremer<sup>18</sup> have described a method for extracting adiabatic frequencies from vibrational spectra, which isolate the motions of individual bonds. A nearly equivalent approach involves computing Hooke's Law spring constants for a bond by stretching and compressing it by a small amount (0.025 Å) relative to the equilibrium geometry.<sup>16,19</sup> The Hooke's Law approach does not give force constants identical to those calculated for adiabatic frequencies, because the displacements do not, in general, correspond to a superposition of normal modes (since the center of mass is not constrained to remain stationary in such calculations). Nevertheless, these two approaches do not differ greatly,<sup>19</sup> and Hooke's Law spring constants can more easily be compared among different types of atoms.

Table 2 summarizes DFT results for the isoelectronic series in Scheme 1, compared with experimental stretching force constants, where available, in parentheses. The first two rows summarize the double and single bonds in the unsaturated systems: **3**, isobutene (**6**), and 2-fluoropropene (**9**), respectively. The third row lists results for the trigonal species: **1**, *tert*-butyl cation (**4**), and 2-fluoropropyl cation (**7**). The fourth row lists results for the tetrahedral species.

The spring constant ratios listed in Table 3 provide the focus for the following discussion. The first row of Table 3 compares *sp*<sup>2</sup>–*sp*<sup>2</sup> double-bond with *sp*<sup>2</sup>–*sp*<sup>3</sup> single-bond stretches within the same molecule (**3** and its isoelectronic alkenes), including theory and experiment for the neutral examples. The calculated ratios all have values close to 2, consistent with the notion that a double bond has twice the strength of a single bond (in accord with X-ray studies that show short B=C distances in boron-stabilized carbanions).<sup>7</sup>

The remaining entries use the corresponding *sp*<sup>3</sup>–*sp*<sup>3</sup> spring constants for **2**, for 2-fluoro-2-methylpropane (**5**), and for 2,2-difluoropropane (**8**), respectively, as the denominators of the ratios. The second row of Table 3 compares *sp*<sup>2</sup>–*sp*<sup>3</sup> single

**Table 2.** Spring Constants Calculated at B3LYP/aug-cc-pVTZ in N/m for Bond Stretches in Species 1–9<sup>a</sup>

|                                                 | X = B,<br>Y = CH <sub>3</sub>  | X = C,<br>Y = CH <sub>3</sub>                         | X = C,<br>Y = F                                       |
|-------------------------------------------------|--------------------------------|-------------------------------------------------------|-------------------------------------------------------|
| <i>sp</i> <sup>2</sup> – <i>sp</i> <sup>2</sup> | <i>k</i> <sub>B=C</sub> = 5.59 | <i>k</i> <sub>C=C</sub> = 9.24 (8.23 <sup>17c</sup> ) | <i>k</i> <sub>C=C</sub> = 9.55 (8.95 <sup>17d</sup> ) |
| <i>sp</i> <sup>2</sup> – <i>sp</i> <sup>3</sup> | <i>k</i> <sub>BC</sub> = 2.72  | <i>k</i> <sub>CC</sub> = 4.26 (4.16 <sup>17c</sup> )  | <i>k</i> <sub>CC</sub> = 4.58 (5.10 <sup>17d</sup> )  |
|                                                 | <i>k</i> <sub>BMe</sub> = 3.48 | <i>k</i> <sub>CMe</sub> = 4.65                        | <i>k</i> <sub>CMe</sub> = 4.83                        |
| <i>sp</i> <sup>3</sup> – <i>sp</i> <sup>3</sup> | <i>k</i> <sub>MeB</sub> = 2.51 | <i>k</i> <sub>MeC</sub> = 3.98                        | <i>k</i> <sub>MeC</sub> = 4.18 (4.19 <sup>17b</sup> ) |

<sup>a</sup> Values in parentheses summarize reported force constants derived from experimental vibrational spectra. See text for explanation of symbols.

**Table 3.** Ratios of Spring Constants Calculated at B3LYP/aug-cc-pVTZ<sup>a,b</sup>

|                                                   | X = B, Y = CH <sub>3</sub>    | X = C, Y = CH <sub>3</sub>            | X = C, Y = F                          |
|---------------------------------------------------|-------------------------------|---------------------------------------|---------------------------------------|
| <i>k</i> <sub>X=C</sub> / <i>k</i> <sub>XC</sub>  | 2.06 ( <b>3</b> )             | 2.17 ( <b>6</b> , 1.98 <sup>c</sup> ) | 2.09 ( <b>9</b> , 1.75 <sup>d</sup> ) |
| <i>k</i> <sub>XC</sub> / <i>k</i> <sub>MeX</sub>  | 1.08 ( <b>3</b> vs <b>2</b> ) | 1.07 ( <b>6</b> vs <b>5</b> )         | 1.10 ( <b>9</b> vs <b>8</b> )         |
| <i>k</i> <sub>X=C</sub> / <i>k</i> <sub>MeX</sub> | 2.23 ( <b>3</b> vs <b>2</b> ) | 2.32 ( <b>6</b> vs <b>5</b> )         | 2.28 ( <b>9</b> vs <b>8</b> )         |
| <i>k</i> <sub>XMe</sub> / <i>k</i> <sub>MeX</sub> | 1.39 ( <b>1</b> vs <b>2</b> ) | 1.17 ( <b>4</b> vs <b>5</b> )         | 1.16 ( <b>7</b> vs <b>8</b> )         |

<sup>a</sup> This work. <sup>b</sup> Values in parentheses represent ratios of experimental force constants. <sup>c</sup> From experimentally derived force constants in ref 17c. <sup>d</sup> From experimentally derived force constants in ref 17d.

bonds of the unsaturated systems with the *sp*<sup>3</sup>–*sp*<sup>3</sup> single bonds of the tetrahedral systems. The *sp*<sup>2</sup>–*sp*<sup>3</sup> single bonds are tighter than the *sp*<sup>3</sup>–*sp*<sup>3</sup> bonds, consistent with expectation based on hybridization effects: the greater fraction of *s*-character in the former makes them stiffer. Comparing the unsaturated anion **3** vs the tetrahedral anion **2** gives nearly the same ratio as do comparisons of isobutene (**6**) vs neutral **5** or 2-fluoropropene (**9**) vs neutral **8**.

The third row of Table 3 lists the entries in the first row multiplied by the entries in the second row. The ratio for the double bond in **9** (CH<sub>3</sub>CF=CH<sub>2</sub>) versus the single bond in **8** ((CH<sub>3</sub>)<sub>2</sub>CF<sub>2</sub>) lies halfway between the ratios for **2** vs **3** and **6** vs **5**, with differences on the order of 2%.

An outlying point, *k*<sub>BMe</sub>/*k*<sub>MeB</sub> = 1.39, emerges when the trigonal systems are contrasted. The last row of Table 3 looks at the single bonds in **1** and the isoelectronic carbocations vs the *sp*<sup>3</sup>–*sp*<sup>3</sup> single bonds in the respective tetrahedral species. The ratio for *tert*-butyl cation (**4**) vs *tert*-butyl fluoride (**5**) has a value nearly the same as for cation **7** vs neutral 2,2-difluoropropane (**8**), but the spring constant for **1** exhibits a much greater value (relative to the corresponding *sp*<sup>3</sup>–*sp*<sup>3</sup> single bond in the tetrahedral anion) than do the cations or do examples previously discussed.<sup>2,3</sup>

Gas phase spectroscopy validates the computational level used here. The calculated spring constant ratios exclude effects of solvation, packing forces, or counterions. They indicate that electronegativity and hyperconjugation act together for **1** vs **2** to give a larger ratio than is found in comparing carbocations with saturated neutral molecules.

**Acknowledgment.** The authors thank the FELIX staff, in particular Drs. Britta Redlich and Lex van der Meer. This work is part of the research program of FOM and was supported by NSF Grant CHE0848517.

**Note Added after ASAP Publication.** This paper was published on the Web on June 28, 2010, with a misplaced radical in eq 1. The corrected version was reposted on June 30, 2010.

**Supporting Information Available:** Anharmonic frequencies computed for **1**–**3**, labeled spectra, and full ref 12. This material is available free of charge via the Internet at <http://pubs.acs.org>.

(18) Kraka, E.; Cremer, D. *ChemPhysChem* **2009**, *10*, 686–698.

(19) Oomens, J.; Kraka, E.; Nguyen, M. K.; Morton, T. H. *J. Phys. Chem. A* **2008**, *112*, 10774–10783.